Chromatic Adaptation Performance of Different RGB Sensors

Sabine Süsstrunk[a,c], Jack Holm[b], Graham D. Finlayson[c]

(a) Communication Systems Department, Swiss Federal Institute of Technology (EPFL), Lausanne, Switzerland
(b) Hewlett-Packard Laboratories, Palo Alto, U.S.A.
(c) School of Information Systems, University of East Anglia, Norwich, U.K.

ABSTRACT

Chromatic adaptation transforms are used in imaging systems to map image appearance to colorimetry under different illumination sources. In this paper, the performance of different chromatic adaptation transforms (CAT) is compared with the performance of transforms based on RGB primaries that have been investigated in relation to standard color spaces for digital still camera characterization and image interchange. The chromatic adaptation transforms studied are von Kries, Bradford, Sharp, and CMCCAT2000. The RGB primaries investigated are ROMM, ITU-R BT.709, and "prime wavelength" RGB. The chromatic adaptation model used is a von Kries model that linearly scales post-adaptation cone responses with illuminant dependent coefficients. The transforms were evaluated using 16 sets of corresponding color data. The actual and predicted tristimulus values were converted to CIELAB, and three different error prediction metrics, ΔE_{Lab}, ΔE_{CIE94}, and $\Delta E_{CMC(1:1)}$ were applied to the results. One-tail Student-t tests for matched pairs were calculated to compare if the variations in errors are statistically significant. For the given corresponding color data sets, the traditional chromatic adaptation transforms, Sharp CAT and CMCCAT2000, performed best. However, some transforms based on RGB primaries also exhibit good chromatic adaptation behavior, leading to the conclusion that white-point independent RGB spaces for image encoding can be defined. This conclusion holds only if the linear von Kries model is considered adequate to predict chromatic adaptation behavior.

Keywords: chromatic adaptation transform (CAT), von Kries, sharp transform, Bradford transform, CMCCAT2000, ROMM RGB, prime wavelength RGB, ITU-R BT.709, equi-energy RGB, corresponding color data

1. CHROMATIC ADAPTATION

Adaptation can be considered as a dynamic mechanism of the human visual system to optimize the visual response to a particular viewing condition. Dark and light adaptation are the changes in visual sensitivity when the level of illumination is decreased or increased, respectively. Chromatic adaptation is the ability of the human visual system to discount the color of the illumination and to approximately preserve the appearance of an object. It can be explained as independent sensitivity regulation of the three cone responses. Chromatic adaptation can be observed by examining a white object under different types of illumination, such as daylight and incandescent. Daylight is "bluer": it contains far more short-wavelength energy than incandescent. However, the white object retains its white appearance under both light sources, as long as the viewer is adapted to the light source.

Image capturing systems, such as scanners and digital cameras, do not have the ability to adapt to an illumination source. Scanners usually have fluorescent light sources with correlated color temperatures around 4200 to 4800 Kelvin. Illumination sources captured by digital cameras vary according to the scene, and often within the scene. Additionally, images captured with these devices are viewed using a wide variety of light sources. Common white-point chromaticities for monitor viewing are D50, D65, and D93. Hardcopy output is usually evaluated using standard illuminant D50 simulators. To faithfully reproduce the appearance of image colors, it follows that all image processing systems need to apply a transform that converts the input colors captured under the input illuminant to the corresponding output colors under the output illuminant. This can be achieved by using a *chromatic adaptation transform*. Basically, applying a chromatic adaptation transform to the tristimulus values (X', Y', Z') of a color under one adapting light source predicts the corresponding color's tristimulus values (X", Y", Z") under another adapting light source.

2. CHROMATIC ADAPTATION TRANSFORMS

There are several chromatic adaptation transforms described in the literature, most based on the von Kries model [1]. CIE tristimulus values are linearly transformed by a 3x3 matrix **M** to derive post-adaptation cone responses under the first illuminant, denoted as R'G'B' in this paper. The values of **M** are transform dependent. The resulting R'G'B' values are independently scaled to get the post-adaptation cone responses R"G"B" under the second illuminant. The scaling coefficients are also transform dependent, but most often based on the illuminants' white-point post-adaptation cone responses. If there are no non-linear coefficients, this transform can be expressed as a diagonal matrix. To obtain CIE tristimulus values (X"Y"Z") under the second illuminant, the R"G"B" are then multiplied by $\mathbf{M}^{-1}$, the inverse of matrix **M**. Equation (1) describes a matrix notation of this concept:

$$\begin{bmatrix} X'' \\ Y'' \\ Z'' \end{bmatrix} = [\mathbf{M}_{\mathrm{CAT}}]^{-1} * \begin{bmatrix} R''_w / R'_w & 0 & 0 \\ 0 & G''_w / G'_w & 0 \\ 0 & 0 & B''_w / B'_w \end{bmatrix} * [\mathbf{M}_{\mathrm{CAT}}] * \begin{bmatrix} X' \\ Y' \\ Z' \end{bmatrix} \qquad (1)$$

Quantities R'_w, G'_w, B'_w and R''_w, G''_w, B''_w are computed from the tristimulus values of the first and second illuminants, respectively, by multiplying the corresponding XYZ vectors by $\mathbf{M}_{\mathrm{CAT}}$.

Following is a description of the four chromatic adaptation transforms that are used for the comparisons described later in this paper. It should be noted that all comparisons are based on the von Kries chromatic adaptation model as outlined in equation (1). Therefore, full adaptation by the human observer is assumed. Partial adaptation, as can be taken into account with other chromatic adaptation transform models, such as CMCCAT2000 [2], CMCCAT97 [3], or RLAB [4], is not taken into consideration.

1. The Von Kries Chromatic Adaptation Transform (von Kries CAT)

A clear distinction has to be made between the von Kries *adaptation model* as described above and the von Kries *chromatic adaptation*. The von Kries CAT assumes that chromatic adaptation is indeed an independent gain control of the cone responses of the human visual system, and that the scaling is based on the ratio of the cone responses of the illuminants. Under this assumption, the matrix **M** of equation (1) needs to linearly transform tristimulus values (XYZ) into relative cone responses (LMS). Typically, the cone responses are determined from the tristimulus values using the following matrix by Hunt, Pointer and Estevez [4].

$$\mathbf{M}_{\text{von Kries}} = \begin{bmatrix} 0.3897 & 0.6890 & -0.0787 \\ -0.2298 & 1.1834 & 0.0464 \\ 0 & 0 & 1 \end{bmatrix}$$

2. Bradford Chromatic Adaptation Transform (BFD CAT)

A widely used newer chromatic adaptation transform is the Bradford transform. It was empirically derived by Lam from a set of corresponding colors as determined from 58 dyed wool samples with varying color constancy, evaluated under illuminants A and D65 [5]. Because of the varying color constancy of the samples, the experiment was designed so that corresponding colors represented the same appearance under the different illumination sources, and not necessarily the same sample. The original Bradford chromatic adaptation transform is a modified Nayatani transform [6] and contains a non-linear correction in the blue region. In many applications, this non-linearity is neglected [7]. The resulting linearized Bradford CAT is then as written in equation (1), using the following transform matrix $\mathbf{M}_{\mathrm{BFD}}$. For the experiments in this paper, the linearized version of the transform was used, and subsequent mentioning of the BFD CAT always refers to its linear form.

$$\mathbf{M}_{\mathrm{BFD}} = \begin{bmatrix} 0.8951 & 0.2664 & -0.1614 \\ -0.7502 & 1.7135 & 0.0367 \\ 0.0389 & -0.0685 & 1.0296 \end{bmatrix}$$

3. The Sharp Transform (Sharp CAT)

One implication of the Bradford chromatic adaptation transform is that color correction for illumination takes place not in cone space but rather in a 'narrowed' cone space. The Bradford sensors (the linear combination of XYZs defined in the Bradford transform) have their sensitivity more narrowly concentrated than the cones (see Figure 1). Additionally, the long

and medium wavelength Bradford sensitivities are more de-correlated. However, Bradford sensors are not optimally narrow. Recent research [8] has shown that a chromatic adaptation transform based on even sharper sensors performs just as well as the Bradford transform for sets of corresponding color data, and in some cases even better than its linearized form.

The transformation matrix $\mathbf{M}_{\text{Sharp}}$ used for the comparisons in this paper is based on white-point preserving data-based sharpening of Lam's corresponding color data set [8], and is as follows:

$$\mathbf{M}_{\text{Sharp}} = \begin{bmatrix} 1.2694 & -0.0988 & -0.1706 \\ -0.8364 & 1.8006 & 0.0357 \\ 0.0297 & -0.0315 & 1.0018 \end{bmatrix}$$

It should be noted, however, that this matrix $\mathbf{M}_{\text{Sharp}}$ is the result of preliminary studies [8, 9], and future chromatic adaptation research by the authors will in all likelihood result in a modification of the matrix.

4. CMCCAT2000

CMCCAT97 is a chromatic adaptation transform included in the CIECAM97s color appearance model. It is based on the Bradford transform, but includes a step to model partial adaptation [3]. Lately, a simplified chromatic adaptation transform, called CMCCAT2000 [2], has been developed to supersede CMCCAT97. CMCCAT2000 has a new transformation matrix **M** and no non-linear correction in the blue. It also calculates the degree of adaptation differently than the previous version. In this paper, the new transformation matrix of CMCCAT2000 is used with the chromatic adaptation model described in equation (1), and the degree of adaptation is not considered. The new transformation matrix $\mathbf{M}_{\text{CMCCAT}}$ is as follows:

$$\mathbf{M}_{\text{CMCCAT}} = \begin{bmatrix} 0.7982 & 0.3389 & -0.1371 \\ -0.5918 & 1.5512 & 0.0406 \\ 0.0008 & 0.0239 & 0.9753 \end{bmatrix}$$

3. CORRESPONDING COLOR DATA

Corresponding colors can be described as a pair of tristimulus values (X, Y, Z), based on one physical stimulus that appears to be the same color when viewed using two different illumination sources. Chromatic adaptation transform matrices **M**, such as described above, are usually derived by using one or more experimental sets of corresponding color data. and finding the transform that minimizes the perceptual mapping errors. Luo and Hunt have accumulated several such sets from the literature for the purpose of deriving and evaluating color appearance models and chromatic adaptation transforms [10]. They include data sets based on reflective stimuli [5, 11-14], and data sets based on monitor and projected stimuli [15, 16]. The characteristics of the 16 corresponding color data sets used for the performance comparison are summarized in Table 1.

Table 1: Characteristics of the corresponding color data sets used in this study.

Data Set	No. of Samples	Approx. Illuminant		Sample Size	Medium	Experimental Method
		Test	Ref.			
Lam	58	D65	A	L	Refl.	Memory
Helson	59	D65	A	S	Refl.	Memory
CSAJ	87	D65	A	S	Refl.	Haploscopic
Lutchi	43	D65	A	S	Refl.	Magnitude
Lutchi D50	44	D65	D50	S	Refl.	Magnitude
Lutchi WF	41	D65	WF	S	Refl.	Magnitude
Kuo&Luo	40	D65	A	L	Refl.	Magnitude
Kuo&Luo TL84	41	D65	TL84	S	Refl.	Magnitude
Braun&Fairchild 1	17	D65	D93	S	Monitor&Refl.	Matching
Braun&Fairchild 2	16	D65	D93	S	Monitor&Refl.	Matching
Braun&Fairchild 3	17	D65	D30	S	Monitor&Refl.	Matching
Braun&Fairchild 4	16	D65	D30	S	Monitor&Refl.	Matching
Breneman 1	12	D65	A	S	Trans.	Magnitude
Breneman 8	12	D65	A	S	Trans.	Magnitude
Breneman 4	12	D65	A	S	Trans.	Magnitude
Breneman 6	11	D55	A	S	Trans.	Magnitude

4. RGB COLOR SPACES

In many image workflows today, image RGB values have first to be transformed to XYZ before the chromatic adaptation transform can be applied. In other words, image RGB code values are first converted to X'Y'Z' using the appropriate transform, and then are transformed to post-adaptation cone responses R'G'B' under the first illuminant using the linear transform **M**. They then are independently scaled to get the post-adaptation cone responses R"G"B" under the second illuminant, transformed by $\mathbf{M}^{-1}$ to get X"Y"Z" values, and finally converted to image RGB code values appropriate for the second illuminant. In practice, however, the different matrices are often concatenated if the scaling coefficients are known in advance and a linear model, such as described in equation (1), is used for chromatic adaptation.

It is of interest to study if there are RGB color spaces that approximate post-adaptation cone responses. Such RGB spaces can be considered to be white-point independent, because the image RGB values are the post-adaptation cone responses (after linearization, if necessary). From the standpoint of chromatic adaptation, the image RGB values are an appearance description. When transforming these RGB values to the corresponding color XYZ values for a particular adopted white chromaticity, the scaling for the destination adopted white is applied to the matrix that transforms from RGB to XYZ. This matrix is obtained by premultiplying matrix $\mathbf{M}^{-1}$ by the RGB scaling from an equi-energy adopted white to the destination adopted white. Likewise, converting XYZ values for a particular adopted white to the RGB appearance description involves applying the inverse of the matrix which would be used to transform from the RGB values to the adopted white XYZ values.

Color spaces based on the ITU-R BT.709, ROMM, and "prime wavelengths" RGB primaries are considered in this paper. These color spaces have been proposed and/or investigated for digital still camera characterization and interchange spaces for color image workflows, where images are viewed under different viewing conditions. If color spaces based on these RGB primaries exhibit such favorable chromatic adaptation behavior as outlined above, it can be assumed that color image processing would become computationally "cheaper," and quantization errors would be minimized.

5. ITU-R BT.709

The latest video RGB standard for the production and exchange of HDTV programming is called ITU-R BT.709 [17]. The 709 primaries are practically the same as the EBU-PAL CCIR 601 primaries, but the 709 standard defines a different form of gamma correction. The 709 primaries match most modern CRT phosphors. sRGB is based on the ITU-R BT.709 primaries [18].

The matrix that transforms CIE 1931 XYZ to ITU-R BT.709 is:

$$\mathbf{C} = \begin{bmatrix} 3.2410 & -1.5374 & -0.4986 \\ -0.9692 & 1.8760 & 0.0416 \\ 0.0556 & -0.2040 & 1.0570 \end{bmatrix}$$

However, the row sums of this matrix are not all equal to unity. This means that the matrix is not white point preserving. A transformation that results in equi-energy RGB has to be derived. This is accomplished by inverting matrix **C**, divide each coefficient of the inverted matrix by its row sum, and then invert to produce the white point preserving XYZ to RGB matrix [19]. Therefore, the CIE 1931 XYZ to equi-energy 709 RGB matrix is as follows:

$$\mathbf{M}_{709} = \begin{bmatrix} 3.0803 & -1.5373 & -0.5430 \\ -0.9211 & 1.8758 & 0.0453 \\ 0.0528 & -0.2040 & 1.1511 \end{bmatrix}$$

6. ROMM/RIMM RGB

ROMM (Reference Output Medium Metric) RGB is a wide-gamut, rendered RGB color space [20]. It was designed by Eastman Kodak and is intended as an RGB color space for manipulating and editing images after the initial rendering has been applied. The ROMM RGB primaries are not tied to any monitor specification. They were selected to wholly enclose an experimentally-determined gamut of surface colors, so that there is no loss of color information when representing reflectance colors that have been captured in an unrendered color space. The corresponding unrendered color space proposed by Eastman Kodak, RIMM (Reference Input Medium Metric) RGB, has the same primaries. The XYZ to equi-energy ROMM RGB matrix $\mathbf{M}_{\mathrm{ROMM}}$, derived as described above, is as follows:

$$\mathbf{M}_{\text{ROMM}} = \begin{bmatrix} 1.2977 & -0.2556 & -0.0422 \\ -0.5251 & 1.5082 & 0.0169 \\ 0 & 0 & 1 \end{bmatrix}$$

7. Prime Wavelength RGB

Brill et al. [21] proposed prime-color wavelengths of 450, 540, and 605 nm. They proved that monitor primaries based on these wavelengths induce the largest gamut size, and that these monitors are visually very efficient. Holm et al. [22] used prime wavelengths of 450 nm, 540 nm, and 620 nm, derived from ratio RGB of Smith & Pokorny cones responses [23], for subjective tests to determine the best error minimization criteria in going from a non-colorimetric digital camera analysis space to a scene colorimety estimate. The XYZ to prime wavelength monochromatic RGB matrix $\mathbf{M}_{\text{Prime}}$ is based on the latter wavelengths and is as follows:

$$\mathbf{M}_{\text{Prime}} = \begin{bmatrix} 2.0016 & -0.5576 & -0.4440 \\ -0.7997 & 1.6627 & 0.1371 \\ 0.0089 & -0.0190 & 1.0100 \end{bmatrix}$$

The corresponding color matching functions of the three equi-energy RGBs are illustrated in Figure 2.

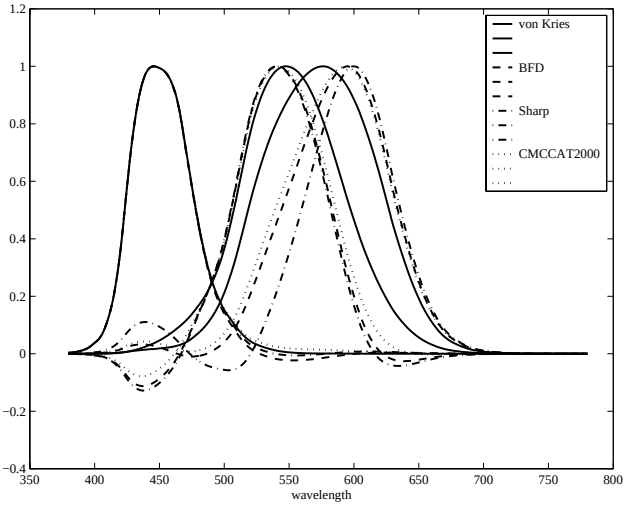

Figure 1: Normalized von Kries, Bradford, Sharp and CMCCAT2000 sensors.

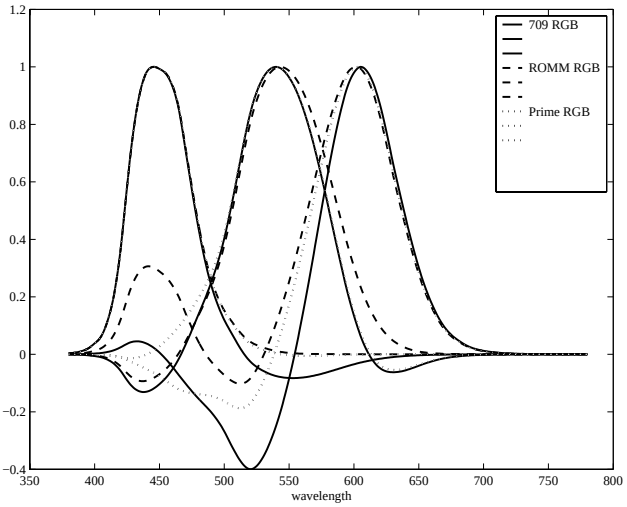

Figure 2: Normalized ROMM RGB, 709 RGB and prime wavelength sensors.

5. PERFORMANCE COMPARISON

Predicted tristimulus values were calculated for the reference illuminants of all corresponding color data sets listed in Table 1, using equation (1) and substituting matrix **M** according to the chromatic adaptation transform tested. The actual and predicted XYZ values were then converted to CIELAB space. Three perceptual error prediction methods, ΔE_{Lab}, ΔE_{CIE94}, and $\Delta E_{CMC(1:1)}$ were applied. One-tail Student-t tests for matched pairs [24] were used to compare if the variations in errors are statistically significant. The resulting *p*-values were calculated using the best performing transformation as one input, and the other transformations of a given data set as the other input. The null hypothesis was that the mean of the difference between the best performing transformation and the other transformation is equal to zero. A large *p*-value supports this hypothesis, and a small *p*-value rejects it. *p*-values equal and larger than 0.01 indicate that the means are equal (or that the null hypothesis cannot be rejected) at a confidence level of 99 percent.

The results for each error prediction method, corresponding color data set, and transform are listed in Tables 3-5 in the Appendix. Table 2 lists the number of times a transform performed best or was statistically the same as the best transform at a 99 percent confidence level. The maximum score for each error metric is 16, as 16 corresponding color data sets were tested.

Table 2: The number of times a transform performed best or was statistically the same (99 percent confidence) as the best transform.

Error Metric	Sharp	BFD	CMCCAT	Von Kries	ROMM	Prime	709RGB
ΔE_{Lab}	16	14	16	6	9	3	7
ΔE_{CIE94}	15	13	15	7	10	3	3
$\Delta E_{CMC(1:1)}$	14	12	15	7	10	4	8

6. CONCLUSIONS

The “traditional” chromatic adaptation transforms, such as the Sharp CAT and CMCCAT2000, outperform the other transforms. This is not so surprising in case of CMCCAT 2000, which was derived from the same corresponding color data sets as was used in this study. The Sharp transform, however, was derived using just the Lam data set, indicating that the set is a good predictor of the others. The Bradford transform also performed quite well, as did equi-energy ROMM RGB. The von Kries CAT did not. The von Kries sensors have distinctly different peaks for the green and red sensors, which leads to the conclusion that chromatic adaptation is not just a function of the cone responses of the human visual system.

Comparing the different sensors in Figure 1, it can be seen that Sharp, CMCCAT2000, and Bradford, as well as ROMM RGB, 709 RGB, and Prime RGB all have their peaks at approximately the same wavelengths. They differ in the slope for the green and red sensors, and in the amount of negative response. Considering the varying, but still occasionally good performance of these sensors, it can be concluded that there might be a number of other RGB sensors that perform just as well as the ones tested here, using the same von Kries chromatic adaptation model and data sets. Any image encoded with such sensors is white-point independent. Such an encoding would facilitate image interchange—chromatic adaptation is probably the most important single image appearance phenomenon that needs to be modeled to achieve good quality image output.

On the other hand, the linear von Kries model used here might be too much of a simplification. While the prediction errors varied according to the data set, none of the transforms was capable to achieve an error that approaches zero. It can be assumed that a non-linear model might better predict chromatic adaptation behavior of the human visual system, and that the ultimate model has not yet been found.

Considering that the premise of this research is image workflows, and the corresponding color data sets were based on single stimuli, with the exception of the Braun&Fairchild sets, it is still necessary to test if the findings also hold true for predicting the appearance of images under different illuminants.

7. REFERENCES

1. J. von Kries, "Chromatic Adaptation," *Festschrift der Albrecht-Ludwigs-Universität*, 1902 [Translation: D.L. MacAdam, "Colorimetry-Fundamentals," *SPIE Milestone Series*, Vol. MS 77, 1993].
2. C. Li, M.R. Luo, B.Rigg, "Simplification of the CMCCAT97," *Proc. IS&T/SID 8th Color Imaging Conference,* to be published November 2000.
3. M.R. Luo, R.W.G. Hunt, "A Chromatic Adaptation Transform and a Colour Inconstancy Index," *Color Res Appl*, Vol. 23, pp. 154–158, 1998.
4. M.D. Fairchild, *Color Appearance Models,* Addison-Wesley, Reading, MA, (1998).
5. K.M. Lam, "Metamerism and Colour Constancy," Ph.D. Thesis, *University of Bradford,* 1985.
6. Y. Nayatani, K. Takahama, and H. Sobagaki, "Formulation of a nonlinear Model of Chromatic Adaptation," *Color Res. Appl.,* Vol. 6, p. 161, 1981.
7. S. Swen and L. Wallis, "Chromatic Adaptation Tag Proposal," *ICC Votable Proposal Submission,* No. 8.2, June 9, 2000.
8. G.D. Finlayson and S. Süsstrunk, "Performance of a Chromatic Adaptation Transform based on Spectral Sharpening," *Proc. IS&T/SID 8th Color Imaging Conference,* to be published November 2000.
9. G.D. Finlayson and S. Süsstrunk, "Spectral Sharpening and the Bradford Transform," *Proc. CIS2000,* pp. 236-243, 2000.
10. M.R. Luo and P.A. Rhodes, Corresponding Colour Data Sets, *University of Derby,* <http://colour.derby.ac.uk/colour/info/catweb/>.
11. H. Helson, D.B. Judd, and M.H. Warren, "Object-Color Changes from Daylight to Incandescent Filament Illumination," *Illuminating Eng.,* Vol. 47, p. 221-233, 1952.
12. L. Mori, H. Sobagaki, H. Komatasubara, and K. Ikeda, "Field trials on the CIE chromatic adaptation formula," *Proc. of the CIE 22nd Session,* pp. 55-58, 1991.
13. M. R. Luo, A.A. Clarke, P.A. Rhodes, S.A.R. Scrivener, A. Schappo, and TAIT C.J. Tait, "Quantifying Colour Appearance. Part I. LUTCHI Colour Appearance Data," *Color Res. Appl.,* Vol. 16, pp. 166-180, 1991.
14. W.G. Kuo, M.R. Luo, H.E. Bez, "Various chromatic-adaptation transforms tested using new colour appearance data in textiles," *Color Res. Appl.,* Vol. 21, pp. 313-327, 1995.
15. K.M. Braun and M.D. Fairchild, "Psychophysical generation of matching images for cross-media color reproduction," *Proc. IS&T/SID's 4th Color Imaging Conference,* pp. 214-220, 1996.
16. E.J. Breneman, "Corresponding chromaticities for different states of adaptation to complex visual fields," *J. Opt. Soc. Am.,* Vol. 4, pp. 1115-1129, 1987.
17. ITU-R Recommendation BT.709-3: 1998, *Parameter values for the HDTV standards for production and international programme exchange.*
18. IEC 61966-2-1: 1999. *Multimedia systems and equipment – Colour measurement and management – Part 2-1: Colour management – Default RGB colour space – sRGB.*
19. ISO 17321, WD 4, Graphic Technology and Photography – *Colour characterisation of digital still cameras (DSCs) using colour targets and spectral illumination,* November 1999.
20. K.E. Spaulding, G.J. Woolfe, E.J. Giorgianni, "Image States and Standard Color Encodings (RIMM/ROMM RGB)," *Proc. IS&T/SID 8th Color Imaging Conference,* to be published November 2000.
21. M.H. Brill, G.D. Finlayson, P.M. Hubel and W.A Thornton, "Prime Colours and Colour Imaging," *Proc. IS&T/SID 6th Color Imaging Conference,* pp. 33-42, 1998.
22. J. Holm, I. Tastl, S. Hordley, "Evaluation of DSC (Digital Still Camera) Scene Analysis Error Metrics - Part 1," *Proc. IS&T/SID 8th Color Imaging Conference,* to be published November 2000.
23. V. C. Smith and J. Pokorny, "Spectral sensitivity of colorblind observers and the cone pigments," *Vision Research*, Vol. 12, pp. 2059-2071, 1972.
24. R.E. Walpole, R.H. Myers, S.L. Myers, *Probability and Statistics for Engineers and Scientists,* 6th Ed., Prentice Hall International, Upper Saddle River, NJ, 1998.

8. APPENDIX

Table 3: RMS and meand ΔE color difference of actual and predicted appearance, bold *p*-values indicate that there is 99 percent confidence that the transform performs as well as the best transform for a given data set.

Lam Data Set	**Sharp**	**BFD**	**CMCCAT**	von Kries	ROMM	Prime	709RGB
RMS ΔE	**5.1**	**5.3**	**5.2**	7.7	6.6	8.8	43.8
mean Δ E	**4.5**	**4.4**	**4.5**	6.5	5.7	7.4	21.1
p-value	**0.4615**	**n/a**	**0.3342**	0.0000	0.0001	0.0000	0.0007

Table 3: cont.

Helson	**Sharp**	**BFD**	**CMCCAT**	von Kries	ROMM	Prime	709RGB
RMS ΔE	**6.1**	**6.7**	**6.1**	8.1	8.0	8.9	45.9
mean ΔE	**5.3**	**5.5**	**5.3**	6.9	7.2	7.6	21.2
p-value	**0.4778**	**0.2457**	**n/a**	0.0003	0.0000	0.0000	0.0021

CSAJ	**Sharp**	**BFD**	**CMCCAT**	von Kries	ROMM	Prime	709RGB
RMS ΔE	**5.6**	**5.9**	**5.6**	7.5	6.3	8.8	18.3
mean ΔE	**5.1**	**5.4**	**5.2**	6.6	5.8	7.8	13.3
p-value	**n/a**	**0.0249**	**0.2903**	0.0000	0.0000	0.0000	0.0000

Lutchi	**Sharp**	**BFD**	**CMCCAT**	**von Kries**	ROMM	Prime	709RGB
RMS ΔE	**7.6**	**7.6**	**6.7**	**8.4**	8.8	11.0	56.0
mean ΔE	**6.8**	**6.9**	**6.0**	**7.1**	7.5	10.2	39.5
p-value	**0.0263**	**0.0122**	**n/a**	**0.0395**	0.0079	0.0000	0.0000

Lutchi D50	**Sharp**	BFD	**CMCCAT**	**von Kries**	ROMM	**Prime**	**709RGB**
RMS ΔE	**6.8**	6.9	**6.6**	**6.6**	7.4	**6.6**	**8.3**
mean ΔE	**6.3**	6.3	**6.0**	**5.8**	6.9	**5.9**	**7.0**
p-value	**0.0165**	0.0017	**0.1250**	**n/a**	0.0019	**0.4210**	**0.0320**

LutchiWF	**Sharp**	BFD	**CMCCAT**	von Kries	**ROMM**	Prime	709RGB
RMS ΔE	**8.7**	9.9	**8.5**	11.7	**8.4**	14.1	26.1
mean ΔE	**7.8**	8.9	**7.5**	10.6	**7.4**	12.8	20.8
p-value	**0.0697**	0.0008	**0.3644**	0.0000	**n/a**	0.0000	0.0000

Kuo&Luo	**Sharp**	**BFD**	**CMCCAT**	von Kries	ROMM	Prime	709RGB
RMS ΔE	**7.7**	**7.0**	**8.3**	10.2	8.0	11.4	64.1
mean ΔE	**6.9**	**6.4**	**7.3**	9.1	7.4	10.3	39.2
p-value	**0.0782**	**n/a**	**0.0387**	0.0000	0.0009	0.0000	0.0001

Kuo&Luo TL84	**Sharp**	**BFD**	**CMCCAT**	von Kries	**ROMM**	Prime	709RGB
RMS ΔE	**4.7**	**5.0**	**4.9**	6.4	**4.7**	7.4	11.1
mean ΔE	**4.3**	**4.6**	**4.4**	5.8	**4.3**	6.8	9.4
p-value	**0.4325**	**0.0757**	**0.3230**	0.0002	**n/a**	0.0000	0.0000

Braun&Fairchild 1	**Sharp**	**BFD**	**CMCCAT**	**von Kries**	ROMM	**Prime**	**709RGB**
RMS ΔE	**4.0**	**3.9**	**3.9**	**4.1**	4.8	**4.4**	**3.7**
mean ΔE	**3.8**	**3.6**	**3.7**	**3.6**	4.5	**3.9**	**3.4**
p-value	**0.0665**	**0.0878**	**0.0286**	**0.1230**	0.0057	**0.0630**	**n/a**

Braun&Fairchild 2	**Sharp**	**BFD**	**CMCCAT**	von Kries	**ROMM**	Prime	**709RGB**
RMS ΔE	**6.6**	**6.6**	**6.7**	6.8	**6.9**	7.1	**6.5**
mean ΔE	**5.9**	**6.0**	**6.1**	6.3	**6.1**	6.6	**5.8**
p-value	**0.4143**	**0.2460**	**0.1233**	0.0030	**0.2211**	0.0011	**n/a**

Braun&Fairchild 3	**Sharp**	**BFD**	**CMCCAT**	von Kries	**ROMM**	Prime	709RGB
RMS ΔE	**7.2**	**7.4**	**7.8**	9.7	**6.6**	11.3	12.4
mean ΔE	**7.1**	**7.1**	**7.5**	9.2	**6.4**	10.7	11.5
p-value	**0.1085**	**0.1395**	**0.0389**	0.0008	**n/a**	0.0003	0.0006

Table 3: cont.

Braun&Fairchild 4	**Sharp**	**BFD**	**CMCCAT**	**von Kries**	**ROMM**	Prime	709RGB
RMS ΔE	**6.0**	**5.8**	**6.2**	**7.0**	**6.4**	7.9	8.4
mean ΔE	**5.9**	**5.7**	**6.0**	**6.7**	**6.1**	7.6	8.0
p-value	**0.0820**	**n/a**	**0.0188**	**0.0139**	**0.1892**	0.0019	0.0026

Breneman 1	**Sharp**	**BFD**	**CMCCAT**	**von Kries**	**ROMM**	Prime	**709RGB**
RMS ΔE	**10.8**	**9.9**	**10.6**	**12.1**	**11.9**	14.2	**61.1**
mean ΔE	**10.5**	**9.1**	**10.1**	**10.7**	**10.7**	13.3	**40.1**
p-value	**0.0615**	**n/a**	**0.1500**	**0.0608**	**0.0702**	0.0005	**0.0272**

Breneman 8	**Sharp**	**BFD**	**CMCCAT**	von Kries	**ROMM**	Prime	**709RGB**
RMS ΔE	**14.0**	**16.1**	**14.0**	19.1	**15.5**	19.9	**63.2**
mean ΔE	**12.0**	**14.0**	**11.8**	16.3	**13.6**	17.9	**43.8**
p-value	**0.2964**	**0.1022**	**n/a**	0.0098	**0.0770**	0.0010	**0.0266**

Breneman 4	**Sharp**	**BFD**	**CMCCAT**	von Kries	**ROMM**	Prime	**709RGB**
RMS ΔE	**14.9**	**17.1**	**15.1**	20.2	**16.4**	20.3	**60.7**
mean ΔE	**12.3**	**14.7**	**12.0**	17.4	**14.5**	17.9	**43.1**
p-value	**0.2683**	**0.0647**	**n/a**	0.0026	**0.0274**	0.0007	**0.0244**

Breneman 6	**Sharp**	**BFD**	**CMCCAT**	**von Kries**	**ROMM**	**Prime**	**709RGB**
RMS ΔE	**8.3**	**8.2**	**7.0**	**8.3**	**9.7**	**10.9**	**43.9**
mean ΔE	**7.9**	**7.7**	**6.8**	**7.4**	**9.2**	**10.0**	**27.1**
p-value	**0.0223**	**0.0953**	**n/a**	**0.3483a**	**0.0371**	**0.0176**	**0.0443**

Table 4: RMS and mean ΔE94 color difference of actual and predicted appearance, bold *p*-values indicates that there is 99 percent confidence that the transform performs as well as the best transform for a given data set.

Lam Data Set	**Sharp**	**BFD**	**CMCCAT**	von Kries	ROMM	Prime	709RGB
RMS ΔE94	**3.4**	**3.5**	**3.6**	5.0	4.1	5.2	13.0
mean ΔE94	**2.9**	**3.0**	**3.0**	4.3	3.6	4.5	9.1
p-value	**n/a**	**0.2258**	**0.1888**	0.0000	0.0001	0.0000	0.0000

Helson	**Sharp**	**BFD**	**CMCCAT**	von Kries	ROMM	Prime	709RGB
RMS ΔE94	**4.0**	**4.2**	**4.2**	5.3	5.2	5.1	13.3
mean ΔE94	**3.4**	**3.5**	**3.6**	4.5	4.7	4.4	9.0
p-value	**n/a**	**0.2451**	**0.1309**	0.0002	0.0000	0.0017	0.0000

CSAJ	**Sharp**	BFD	**CMCCAT**	von Kries	ROMM	Prime	709RGB
RMS ΔE94	**4.1**	4.2	**4.1**	5.2	4.5	5.9	9.3
mean ΔE94	**3.7**	3.8	**3.8**	4.7	4.1	5.3	8.0
p-value	**n/a**	0.0099	**0.2385**	0.0000	0.0000	0.0000	0.0000

Lutchi	**Sharp**	**BFD**	**CMCCAT**	**von Kries**	ROMM	Prime	709RGB
RMS ΔE94	**4.5**	**4.0**	**3.4**	**4.0**	5.0	6.4	19.1
mean ΔE94	**4.0**	**3.7**	**3.1**	**3.5**	4.4	6.0	16.4
p-value	**0.0263**	**0.0122**	**n/a**	**0.0395**	0.0079	0.0000	0.0000

Table 4: cont.

Lutchi D50	Sharp	BFD	CMCCAT	**von Kries**	ROMM	**Prime**	709RGB
RMS ΔE94	4.0	3.9	3.8	**3.6**	4.3	**3.7**	4.2
mean ΔE94	3.6	3.5	3.4	**3.1**	4.0	**3.3**	3.8
p-value	0.0002	0.0000	0.0017	**n/a**	0.0001	**0.0812**	0.0072

LutchiWF	**Sharp**	BFD	**CMCCAT**	von Kries	**ROMM**	Prime	709RGB
RMS ΔE94	**4.2**	4.7	**4.3**	6.2	**4.0**	7.3	10.7
mean ΔE94	**4.0**	4.4	**4.0**	5.6	**3.7**	6.8	9.6
p-value	**0.0636**	0.0032	**0.1513**	0.0001	**n/a**	0.0000	0.0000

Kuo&Luo	**Sharp**	**BFD**	**CMCCAT**	von Kries	**ROMM**	Prime	709RGB
RMS ΔE94	**4.2**	**4.1**	**4.3**	5.8	**4.4**	6.6	21.9
mean ΔE94	**4.0**	**3.9**	**4.0**	5.3	**4.1**	6.1	16.4
p-value	**0.2388**	**n/a**	**0.3314**	0.0000	**0.1456**	0.0000	0.0000

Kuo&Luo TL84	**Sharp**	**BFD**	**CMCCAT**	von Kries	**ROMM**	Prime	709RGB
RMS ΔE94	**2.9**	**3.0**	**2.9**	3.7	**2.9**	4.4	5.5
mean ΔE94	**2.7**	**2.8**	**2.7**	3.3	**2.6**	4.1	5.1
p-value	**0.1166**	**0.0585**	**0.2808**	0.0026	**n/a**	0.0000	0.0000

Braun&Fairchild 1	**Sharp**	**BFD**	**CMCCAT**	**von Kries**	ROMM	**Prime**	**709RGB**
RMS ΔE94	**3.0**	**2.9**	**2.9**	**3.1**	3.4	**3.1**	**2.8**
mean ΔE94	**2.8**	**2.7**	**2.7**	**2.7**	3.3	**2.8**	**2.5**
p-value	**0.0489**	**0.0603**	**0.0309**	**0.0268**	0.0077	**0.0452**	**n/a**

Braun&Fairchild 2	**Sharp**	**BFD**	**CMCCAT**	**von Kries**	**ROMM**	Prime	**709RGB**
RMS ΔE94	**5.2**	**5.2**	**5.2**	**5.2**	**5.3**	5.4	**5.1**
mean ΔE94	**4.5**	**4.5**	**4.6**	**4.7**	**4.6**	4.9	**4.5**
p-value	**0.3941**	**0.2467**	**0.1266**	**0.0106**	**0.2083**	0.0016	**n/a**

Braun&Fairchild 3	**Sharp**	**BFD**	**CMCCAT**	von Kries	**ROMM**	Prime	709RGB
RMS ΔE94	**4.5**	**4.8**	**7.8**	6.2	**4.4**	6.3	7.0
mean ΔE94	**4.3**	**4.5**	**7.5**	6.0	**4.3**	6.1	6.8
p-value	**0.4961**	**0.2432**	**0.0980**	0.0008	**n/a**	0.0019	0.0004

Braun&Fairchild 4	**Sharp**	**BFD**	**CMCCAT**	**von Kries**	**ROMM**	**Prime**	**709RGB**
RMS ΔE94	**4.1**	**4.2**	**4.4**	**5.0**	**4.6**	**4.7**	**5.1**
mean ΔE94	**4.0**	**4.0**	**4.2**	**4.8**	**4.3**	**4.6**	**5.0**
p-value	**n/a**	**0.2597**	**0.0189**	**0.0147**	**0.1658**	**0.0514**	**0.0185**

Breneman 1	**Sharp**	**BFD**	**CMCCAT**	**von Kries**	**ROMM**	Prime	709RGB
RMS ΔE94	**5.9**	**5.6**	**5.5**	**6.5**	**6.5**	7.8	17.3
mean ΔE94	**5.6**	**5.0**	**5.0**	**5.5**	**5.8**	7.2	14.4
p-value	**0.0316**	**0.4276**	**n/a**	**0.2286**	**0.1484**	0.0052	0.0052

Breneman 8	**Sharp**	**BFD**	**CMCCAT**	von Kries	**ROMM**	Prime	709RGB
RMS ΔE94	**7.9**	**8.4**	**7.8**	10.3	**8.0**	11.1	20.1
mean ΔE94	**6.8**	**7.2**	**6.5**	8.5	**6.8**	9.8	17.1
p-value	**0.1671**	**0.0593**	**n/a**	0.0096	**0.2552**	0.0017	0.0061

Table 4: cont.

Breneman 4	**Sharp**	**BFD**	**CMCCAT**	von Kries	**ROMM**	Prime	709RGB
RMS ΔE94	**8.9**	**9.6**	**9.0**	11.6	**9.0**	12.0	20.6
mean ΔE94	**7.2**	**7.9**	**7.1**	9.4	**7.5**	10.3	17.6
p-value	**0.2788**	**0.0347**	**n/a**	0.0031	**0.1936**	0.0015	0.0064

Breneman 6	**Sharp**	**BFD**	**CMCCAT**	**von Kries**	**ROMM**	Prime	709RGB
RMS ΔE94	**4.9**	**4.4**	**4.0**	**4.3**	**5.1**	6.4	13.2
mean ΔE94	**4.7**	**4.2**	**3.9**	**3.7**	**4.9**	5.8	11.1
p-value	**0.1631**	**0.2590**	**0.4103**	**n/a**	**0.0410**	0.0092	0.0067

Table 5: ΔCMC color difference of actual and predicted appearance, bold *p*-values indicate that there is 99 percent confidence that the transform performs as well as the best transform for a given data set.

Lam Data Set	**Sharp**	**BFD**	**CMCCAT**	von Kries	ROMM	Prime	709RGB
RMS ΔCMC	**4.2**	**4.3**	**4.2**	6.0	4.8	6.5	18.1
mean ΔCMC	**3.5**	**3.6**	**3.5**	5.1	4.2	5.5	11.7
p-value	**n/a**	**0.4088**	**0.4979**	0.0000	0.0016	0.0000	0.0000

Helson	**Sharp**	**BFD**	**CMCCAT**	von Kries	ROMM	Prime	709RGB
RMS ΔCMC	**4.7**	**4.9**	**4.7**	6.2	6.0	6.3	18.1
mean ΔCMC	**4.0**	**4.1**	**4.0**	5.2	5.3	5.3	11.5
p-value	**n/a**	**0.2335**	**0.2921**	0.0009	0.0000	0.0008	0.0001

CSAJ	**Sharp**	BFD	**CMCCAT**	von Kries	ROMM	Prime	709RGB
RMS ΔCMC	**4.5**	4.7	**4.5**	6.1	4.9	6.9	11.6
mean ΔCMC	**4.1**	4.3	**4.2**	5.4	4.5	6.2	9.7
p-value	**n/a**	0.0033	**0.1973**	0.0000	0.0000	0.0000	0.0000

Lutchi	Sharp	BFD	**CMCCAT**	**von Kries**	ROMM	Prime	709RGB
RMS ΔCMC	5.2	4.5	**4.0**	**4.7**	5.8	7.0	24.3
mean ΔCMC	4.6	4.2	**3.7**	**4.1**	5.0	6.6	19.7
p-value	0.0000	0.0041	**n/a**	**0.1326**	0.0008	0.0000	0.0000

Lutchi D50	Sharp	BFD	CMCCAT	**von Kries**	ROMM	**Prime**	**709RGB**
RMS ΔCMC	4.4	4.4	4.3	**4.0**	4.9	**3.9**	**4.4**
mean ΔCMC	4.1	4.0	3.9	**3.5**	4.5	**3.6**	**4.0**
p-value	0.0003	0.0001	0.0026	**n/a**	0.0001	**0.3327**	**0.0483**

LutchiWF	**Sharp**	BFD	**CMCCAT**	von Kries	**ROMM**	Prime	709RGB
RMS ΔCMC	**5.2**	6.0	**5.3**	7.8	**4.8**	9.2	13.6
mean ΔCMC	**4.8**	5.5	**4.8**	6.9	**4.4**	8.3	11.9
p-value	**0.0276**	0.0009	**0.0776**	0.0000	**n/a**	0.0000	0.0000

Kuo&Luo	**Sharp**	**BFD**	**CMCCAT**	von Kries	**ROMM**	Prime	709RGB
RMS ΔCMC	**4.9**	**4.7**	**4.9**	6.9	**5.1**	7.6	29.9
mean ΔCMC	**4.6**	**4.4**	**4.5**	6.3	**4.8**	7.0	21.0
p-value	**0.1973**	**n/a**	**0.3116**	0.0000	**0.0368**	0.0000	0.0000

Table 5: cont.

Kuo&Luo TL84	**Sharp**	**BFD**	**CMCCAT**	von Kries	**ROMM**	Prime	709RGB
RMS ΔCMC	**3.5**	**3.6**	**3.5**	4.4	**3.5**	5.0	6.8
mean ΔCMC	**3.1**	**3.3**	**3.2**	4.0	**3.1**	4.7	6.1
p-value	**0.3463**	**0.0924**	**0.3352**	0.0018	**n/a**	0.0000	0.0000

Braun&Fairchild 1	**Sharp**	**BFD**	**CMCCAT**	**von Kries**	ROMM	**Prime**	**709RGB**
RMS ΔCMC	**3.7**	**3.5**	**3.5**	**3.6**	4.4	**3.8**	**3.4**
mean ΔCMC	**3.4**	**3.2**	**3.2**	**3.1**	4.1	**3.3**	**3.0**
p-value	**0.0771**	**0.1300**	**0.1015**	**0.1727**	0.0065	**0.1139**	**n/a**

Braun&Fairchild 2	**Sharp**	**BFD**	**CMCCAT**	von Kries	**ROMM**	Prime	**709RGB**
RMS ΔCMC	**6.4**	**6.4**	**6.4**	6.4	**6.6**	6.6	**6.2**
mean ΔCMC	**5.5**	**5.5**	**5.6**	5.7	**5.7**	6.0	**5.4**
p-value	**0.3361**	**0.2268**	**0.1066**	0.0093	**0.1425**	0.0019	**n/a**

Braun&Fairchild 3	**Sharp**	**BFD**	**CMCCAT**	von Kries	**ROMM**	Prime	709RGB
RMS ΔCMC	**5.7**	**6.0**	**6.2**	8.2	**5.6**	8.8	10.6
mean ΔCMC	**5.4**	**5.8**	**6.0**	8.0	**5.4**	8.5	10.0
p-value	**0.4678**	**0.1927**	**0.0804**	0.0002	**n/a**	0.0004	0.0003

Braun&Fairchild 4	**Sharp**	**BFD**	**CMCCAT**	**von Kries**	**ROMM**	**Prime**	**709RGB**
RMS ΔCMC	**5.3**	**5.3**	**5.4**	**5.9**	**5.7**	**5.9**	**6.7**
mean ΔCMC	**5.0**	**5.0**	**5.1**	**5.6**	**5.2**	**5.7**	**6.4**
p-value	**0.3378**	**n/a**	**0.1347**	**0.0390**	**0.2655**	**0.0545**	**0.0148**

Breneman 1	**Sharp**	**BFD**	**CMCCAT**	**von Kries**	**ROMM**	Prime	**709RGB**
RMS ΔCMC	**7.1**	**6.6**	**6.6**	**7.5**	**7.5**	9.2	**23.6**
mean ΔCMC	**6.7**	**5.9**	**6.0**	**6.6**	**6.8**	8.5	**18.5**
p-value	**0.0344**	**n/a**	**0.3378**	**0.1311**	**0.1056**	0.0015	**0.0125**

Breneman 8	**Sharp**	**BFD**	**CMCCAT**	**von Kries**	**ROMM**	Prime	**709RGB**
RMS ΔCMC	**9.3**	**10.0**	**9.1**	**12.0**	**9.2**	13.2	**26.8**
mean ΔCMC	**7.9**	**8.5**	**7.5**	**10.2**	**7.9**	11.7	**21.7**
p-value	**0.1616**	**0.0617**	**n/a**	**0.0117**	**0.2160**	0.0018	**0.0119**

Breneman 4	**Sharp**	**BFD**	**CMCCAT**	von Kries	**ROMM**	Prime	**709RGB**
RMS ΔCMC	**10.6**	**11.4**	**10.6**	13.7	**10.6**	14.3	**27.3**
mean ΔCMC	**8.5**	**9.5**	**8.3**	11.6	**9.0**	12.5	**22.3**
p-value	**0.3143**	**0.0323**	**n/a**	0.0055	**0.1286**	0.0017	**0.0123**

Breneman 6	**Sharp**	**BFD**	**CMCCAT**	**von Kries**	**ROMM**	**Prime**	**709RGB**
RMS ΔCMC	**6.4**	**5.7**	**5.4**	**5.3**	**6.2**	**7.6**	**17.5**
mean ΔCMC	**5.9**	**5.2**	**4.9**	**4.5**	**6.0**	**6.9**	**13.6**
p-value	**0.1487**	**0.2349**	**0.3480**	**n/a**	**0.0273**	**0.0128**	**0.0167**